

铝/铜高频感应接触反应钎焊

张洪涛，刘 多，冯吉才，胡乐亮

(哈尔滨工业大学(威海)材料科学与工程学院,威海 264209)

摘 要: 对铝/铜异种金属接头的高频感应接触反应钎焊工艺进行了研究,在非真空条件下借助钎剂的去膜作用,实现了铝和铜的连接,并根据钎剂去膜过程和对接头力学性能的影响规律优化了钎剂组分。同时借助扫描电镜和能谱分析等分析手段,详细分析了接头的界面结构与物相组成。结果表明,试验中配制的钎剂 65%  $\text{ZnCl}_2$  + 10%  $\text{NaCl}$  + 25%  $\text{NH}_4\text{Cl}$  钎焊效果较好,钎缝厚度约为 80  $\mu\text{m}$ ,钎缝主要由铝基固溶体和化合物  $\text{Al}_2\text{Cu}$  弥散相组成,有大量的 Zn 元素和 Na 元素扩散进入钎缝,接头抗剪强度可以达到 58 MPa。

关键词: 铝合金; 紫铜; 接触反应钎焊; 界面结构

中图分类号: TG454 文献标识码: A 文章编号: 0253-360X(2012)03-0089-04



张洪涛

0 序 言

目前在海洋开发、石油化工、电子仪表、空间技术及军事工程等方面,经常遇到铜与铝、铜与铝合金、铝与铜合金或者铜合金与铝合金的焊接结构,应用极其广泛<sup>[1]</sup>。采用钨极氩弧焊焊接铜和铝时<sup>[2]</sup>,填丝材料选择纯铝,电弧主要熔化铝一侧,而对铜一侧不能熔化太多,最终获得的接头强度和塑性比较低。西北大学安志斌<sup>[3]</sup>对铜和铝激光焊做了许多研究,分析了激光器的功率密度、脉冲波形、脉冲宽度,聚焦透镜离焦量、焦距等因素对焊接质量的影响。常规摩擦焊和搅拌摩擦焊都可以用于铜与铝的焊接<sup>[4-6]</sup>。高温摩擦焊时,高速旋转的接触面温度可达到铝的熔点,完全超出共晶点温度,获得的接头性能较差,易于断裂,主要原因是接触面温度过高,产生了过量的脆性相  $\text{CuAl}_2$  和  $\text{Cu}_9\text{Al}$  相,使接头脆性增大。钎焊由于加热温度一般远低于母材的熔点,因而对母材的物理化学性能通常没有明显的不利影响,因此比较适于异种金属的连接<sup>[7]</sup>。

在此背景下,文中以实现铜和铝的连接为目的,开展铜和铝合金高频感应接触反应钎焊连接的研究。试验中采用 3 种不同钎剂进行钎焊,对各种钎剂的焊接效果进行对比研究,分析了接头界面结构特点,测试了接头的力学性能,优化了焊接工艺。

1 试验方法

试验母材为紫铜和 6063 铝合金,采用线切割将紫铜和 6063 铝合金切成 6 mm × 6 mm × 2 mm 和 10 mm × 10 mm × 3 mm 的试块,然后如图 1 所示进行搭接。焊接前首先去除铝合金表面的油污,然后将工件浸入 60  $^{\circ}\text{C}$ 、质量分数为 10% 的  $\text{NaOH}$  溶液中碱洗 20 s 后取出,并用清水冲洗干净;最后将工件浸入质量分数为 20% 的  $\text{HNO}_3$  溶液中亮蚀 30 s 取出,用清水冲洗干净,并用吹风机吹干备焊。对于紫铜则用 200 号、400 号、600 号水砂纸逐级磨光,然后放在丙酮里用超声波清洗 10 min。按照自上而下(铜/铝)的顺序叠放试块进行焊接。

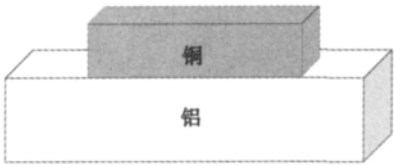


图 1 钎焊试件的接头形式

Fig. 1 Joint of brazing specimens

高频感应钎焊设备采用 SP-30AB 型水冷自控分体式高频感应加热设备,设备输入电压为三相 380 V,50 ~ 60 Hz,最大输出功率为 30 kW。感应圈为紫铜管绕制,工作时紫铜管内通冷却水,实现对高频电源及感应圈的循环水冷。

试验中采用钎剂去除合金表面的氧化膜并对焊接过程进行保护,表 1 为试验配制钎剂的化学组分.

表 1 钎剂组分及熔点  
Table 1 Compositions and melting point of flux

|     | 钎剂化学组成   | 熔点 $T/^\circ\text{C}$ |
|-----|--|-----------------------|
| 1 号 | 95% $\text{ZnCl}_2$ + 5% $\text{NaF}$  | 390                   |
| 2 号 | 65% $\text{ZnCl}_2$ + 10% $\text{NaCl}$ + 25% $\text{NH}_4\text{Cl}$                     | 225                   |
| 3 号 | 55% $\text{ZnCl}_2$ + 28% $\text{SnCl}_2$ + 2% $\text{NaF}$ + 15% $\text{NH}_4\text{Br}$ | 160                   |

通过初步试验,采用电流为 35 A,加热 14 s 可以使焊件表面温度达到  $600\text{ }^\circ\text{C} \pm 10\text{ }^\circ\text{C}$ ;采用电流为 25 A,加热 32 s 可以使焊件表面温度达到  $580\text{ }^\circ\text{C} \pm 10\text{ }^\circ\text{C}$ ;采用电流为 40 A,加热 14 s 可以使焊件表面温度达到  $620\text{ }^\circ\text{C} \pm 10\text{ }^\circ\text{C}$ . 当电流为 25 A 时,加热速度过慢,铝合金在长时间加热过程中很容易产生氧化膜;当电流为 40 A 时,加热速度过快,造成焊件受热严重不均,内外温度差大,必定对钎焊造成不利影响. 因此试验主要选取适中电流为 35 A 进行加热.

2 试验结果与分析

2.1 连接强度

在 INSTRON-5500 电子万能试验机上测试 1 号, 2 号及 3 号钎剂辅助条件下钎焊接头室温抗剪强度,加载速度为 0.5 mm/min. 钎焊时加热电流为 35 A,钎焊温度约为  $600\text{ }^\circ\text{C} \pm 10\text{ }^\circ\text{C}$ . 测试结果显示,采用 1 号钎剂钎焊,接头抗剪强度达到 40 MPa,低于 2 号钎剂钎焊接头的 58 MPa,高于 3 号钎剂钎焊接头的 23 MPa.

2.2 界面组织结构

对 1 号和 2 号钎剂辅助条件下获得的接头界面结构进行分析,由于 3 号钎剂辅助条件下获得的接头抗剪强度过低,不具有实用价值,因此未进行相关分析. 1 号钎剂的成分是 95%  $\text{ZnCl}_2$  + 5%  $\text{NaF}$ ,钎焊时发现钎剂完全熔化后产生少量白烟,焊后不容易清洗. 1 号钎剂辅助钎焊钎缝整体形貌和微观组织形貌如图 2 所示.

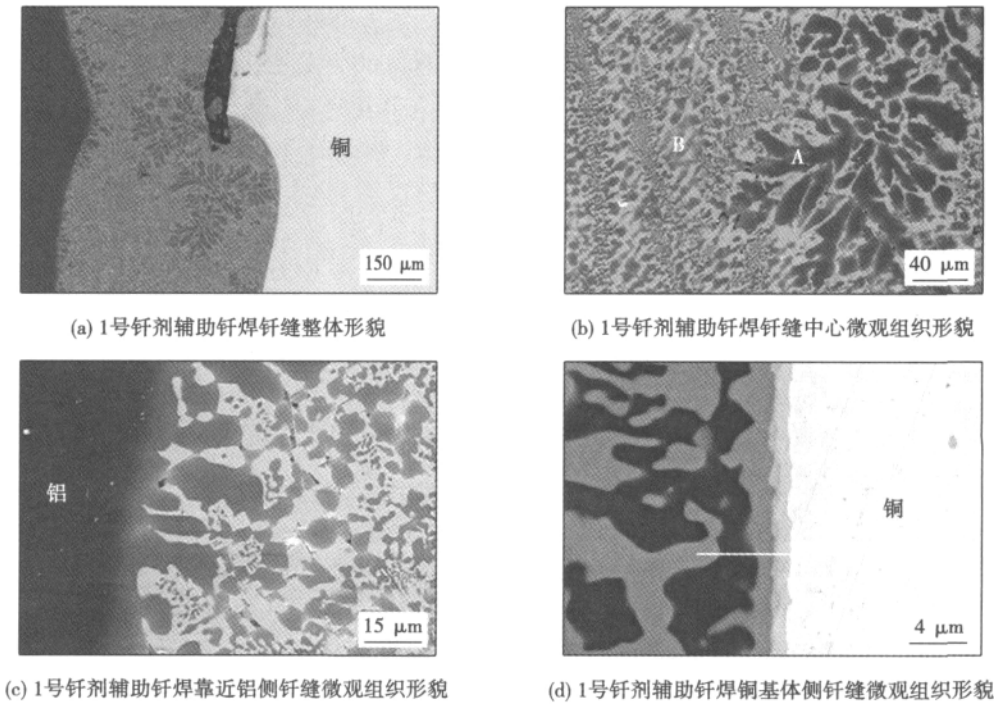


图 2 1 号钎剂辅助焊接接头界面 SEM 形貌  
Fig. 2 SEM morphology of interface of welded joint with No. 1 flux

图 2a 为钎缝整体组织形貌,钎缝厚度约为 500  $\mu\text{m}$ ,黑色物质区域是夹渣. 从图 2b 钎缝中心 400 倍微观组织形貌可以看出钎缝主要是由共晶组织和少量叶状的黑体成分,为了进一步确定钎缝的组成,对图 2b 中 A 点和 B 点进行能谱分析,结果如表 2

所示. A 点主要组分是 Al 元素,还有少量 F,Na,Cl 和 Cu 元素.

图 2c 为靠近铝合金侧微观组织形貌,可以看出铝基体与钎缝之间无其它反应层出现,直接与共晶层相连. 图 2d 为铜基体侧界面微观组织形貌,从

表 2 特征点能谱分析(原子分数, %)

Table 2 Energy spectrum analysis of feature point

|     | F    | Na   | Al    | Cl   | Sn   | Cu    | Zn   |
|-----|------|------|-------|------|------|-------|------|
| A 点 | 0.20 | 4.85 | 88.23 | 0.10 | 0.07 | 3.09  | 3.47 |
| B 点 | 0.99 | 0    | 65.06 | 0.27 | 0.23 | 31.45 | 2.01 |

图 2d 中可见铜基体与钎缝之间除了共晶组织外还有其它反应层,沿图 2d 中直线进行元素线扫描分析,得到结果如图 3 所示. 钎缝反应层到铜基体过渡时,Al 元素含量的变化总体呈现阶梯状,含量逐渐降低,最左侧铝为主要存在元素,最右侧 Al 元素则是微量. 每个相层中含量稳定,相层之间过渡时则呈现较为陡峭的过渡形式. Cu 元素含量分布的变化曲线与 Al 元素基本上呈镜像状态,钎缝层内 Cu 元素含量较低,向铜基体过渡,含量逐渐增加.

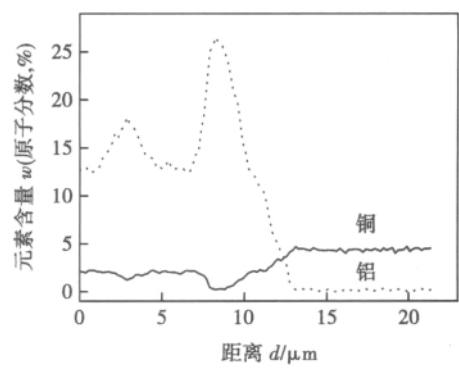


图 3 线扫描结果  
Fig. 3 Result of line scanning

2 号钎剂是 65% ZnCl<sub>2</sub> + 10% NaCl + 25% NH<sub>4</sub>Cl, 钎焊时发现钎剂完全熔化后产生大量白烟,焊后容易清洗. 2 号钎剂辅助钎焊钎缝整体形貌和微观组织形貌如图 4 所示.

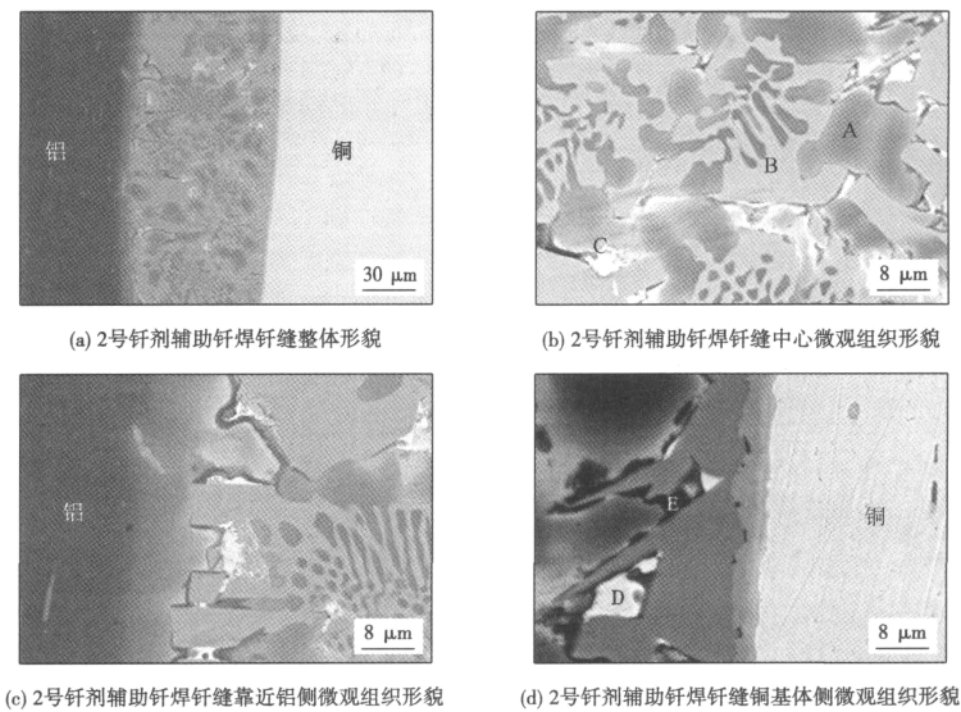


图 4 2 号钎剂辅助焊接接头界面 SEM 形貌  
Fig. 4 SEM morphology of interface of welded joints with No.2 flux

图 4a 为钎缝整体组织形貌,钎缝厚度约为 80 μm 左右. 图 4b 为钎缝中心微观组织形貌,选取特征点进行能谱分析,结果见表 3. A 点区域主要成分是铝基固溶体,有大量的 Zn 和 Na 元素扩散进入基体;B 点区域主要成分是铝铜化合物,从比例判定是 Al<sub>2</sub>Cu 相;C 点区域主要是来自钎剂中的 Na 和 Zn 元素,还有少量 Al、Cu、Cl 和 F 元素扩散进入. 图 4c

为铝侧微观组织形貌,图 4d 为铜基体侧微观组织形貌,可以看出钎缝边缘靠近两侧基体处都有阻碍固态基体向液态金属溶解以及液态金属向固态基体扩散的趋势. 对图 4d 中的特征点进行能谱分析,得到结果见表 4. D 点区域主要成分是氧化物和来自钎剂的 Zn 元素;E 点区域主要是 Al 元素的聚集和来自钎剂中的 Zn 元素,同时也含有部分氧化物.

表 3 钎缝中心能谱分析结果( 原子分数 ,%)

Table 3 Result of energy spectrum analysis in middle of brazing seam

|     | F    | Na    | Al    | Cl   | Sn   | Cu    | Zn    |
|-----|------|-------|-------|------|------|-------|-------|
| A 点 | 0.54 | 22.56 | 61.79 | 0.11 | 0.12 | 2.75  | 12.13 |
| B 点 | 1.52 | 0     | 64.40 | 0.21 | 0.14 | 31.48 | 2.25  |
| C 点 | 0.92 | 59.77 | 3.74  | 0.16 | 0.15 | 5.91  | 29.35 |

表 4 靠近铜侧钎缝特征点能谱分析结果( 原子分数 ,%)

Table 4 Result of energy spectrum analysis in brazing seam near copper side

|     | O     | Cl   | Al    | Cu    | Zn    |
|-----|-------|------|-------|-------|-------|
| D 点 | 28.38 | 8.58 | 6.61  | 10.31 | 46.12 |
| E 点 | 18.29 | 1.20 | 53.08 | 5.71  | 21.73 |

通过上述界面结构分析可见当采用 2 号钎剂进行焊接时,钎剂中的一些元素在焊接过程中可以阻碍铝和铜的接触反应进程,从而减少脆性共晶组织的生成数量,减小钎缝的厚度,显著提高接头的抗剪强度.

3 结 论

(1) 采用配制的钎剂实现了铝和铜接触反应钎焊,钎缝界面结构主要由 Al-Al<sub>2</sub>Cu 共晶组织组成,靠近铝侧钎缝与基体直接连接在一起,而靠近铜侧则在通过一层厚度约为 1 μm 左右的反应层连接,

不同的钎剂对界面结构的总体组成影响不大.

(2) 组分为 65% ZnCl<sub>2</sub> + 10% NaCl + 25% NH<sub>4</sub>Cl 的钎剂钎缝中有大量的 Zn 和 Na 元素扩散进入钎缝,从而可以显著减小界面反应层的厚度,从而提高接头的抗剪强度,接头抗剪强度可以达到 58 MPa.

参考文献:

[1] 李亚江,王 娟,刘 鹏. 异种难焊材料的焊接及应用[M]. 北京: 化学工业出版社,2004.

[2] 刘中青. 异种金属焊接技术指南[M]. 北京: 机械工业出版社,1997.

[3] 安志斌. 异种金属材料的激光焊接研究[D]. 西安: 西北大学,2008.

[4] 李亚江. 特殊及难焊材料的焊接[M]. 北京: 化学工业出版社,2003.

[5] Saeid T ,Abdollah-Zadeh A ,Sazgari B. Weldability and mechanical properties of dissimilar aluminum-copper lap joints made by friction stir welding[J]. Journal of Alloys and Compounds ,2010 , 490( 1/2) : 652 – 655.

[6] Liu Peng ,Shi Qingyu ,Wang Wei ,et al. Microstructure and XRD analysis of FSW joints for copper T2/aluminium 5A06 dissimilar materials[J]. Materials Letters ,2008 ,62( 25) : 4106 – 4108.

[7] 黄旺福,黄金刚. 铝及铝合金焊接指南[M]. 长沙: 湖南科学技术出版社,2005.

作者简介: 张洪涛,男,1980 年出生,博士,副教授,硕士研究生导师. 主要从事特种焊接技术及异种金属连接方面的科研和教学工作. 发表论文 10 余篇. Email: hitzht@yahoo.com.cn

of an ultra-high strength X120 pipeline steel was investigated with thermal simulation. Simulated HAZ continuous cooling transformation (SH-CCT) curves showed that the bainitic microstructure was obtained in CG-HAZ in a wide cooling rate range (0.8 – 25 °C/s). Besides bainite, a small proportion of quasi polygonal ferrite formed in CG-HAZ when the cooling rate was lower than 0.8 °C/s whereas a small proportion of martensite formed when the cooling rate was higher than 25 °C/s. Bainite was obtained in the CG-HAZ when the welding heat input was in the range of 12 – 25 kJ/cm. The Vickers hardness of CG-HAZ (276 – 297 HV0.2) and the impact toughness at room temperature (208 – 225 J) was stable. Simulated results indicated that the X120 pipeline steel was suitable for welding with wide heat inputs, which was attributed to the ultra-low carbon design.

**Key words:** ultra-high strength pipeline steel; heat-affected zone; microstructure transformation; bainite; thermal simulation

**Mathematical model and simulation for cutting of pipe tee with root face groove** WANG Qihua, YIN Guofu, XU Lei, HE Saisong (School of Manufacturing Science & Engineering, Sichuan University, Chengdu 610065, China). pp 77 – 80

**Abstract:** Aimed at the groove cutting during the pipe tee manufacturing, this paper compared bevel groove with root face groove, and presented the advantages of root face groove cutting for pipe tee. The principle of root face groove cutting for branch pipe and main pipe was demonstrated, and then the root face groove cutting model was established, based on the bevel groove cutting model. After simulation with AutoCAD VBA programming tools, the models were verified to be reliable and practical. This paper provides a new approach to improve the welding quality and enhance the manufacturing efficiency of pipe tee.

**Key words:** CNC pipe cutting; pipe tee; bevel groove; root face groove

**New half-bridge soft-switching CO<sub>2</sub> inverter welding machine** SHE Zhiting<sup>1</sup>, CAO Da<sup>1</sup>, XIA Fuping<sup>2</sup>, LI Ying<sup>1</sup> (1. College of Electrical and Information Engineering, Hunan University, Changsha 410082, China; 2. Central Research Institute, Sany Group Co., Ltd., Changsha 410100, China). pp 81 – 84

**Abstract:** In order to reduce the switching loss and ripple of output voltage of CO<sub>2</sub> inverter welding machine and realize the digital control, the soft-switching commutation principle of half-bridge DC-DC converter with adding two assistant power switches to DC busline side is analyzed in this paper. Based on ARM-controlled and double closed-loop (current and voltage) control strategy, a full digital CO<sub>2</sub> inverter welding machine is designed. The soft-switching commutation of new half-bridge DC-DC converter is simulated in the Matlab/Simulink environment. The experimental results illustrate that the full digital ARM-controlled new half-bridge soft-switching inverter welding machine has significant advantages over the traditional analog-controlled inverter welding machine, such as low switching loss, low voltage ripple, flexible programming ability and better stability.

**Key words:** CO<sub>2</sub> inverter welding machine; half-bridge DC-DC converter; soft-switching; digital control

**Analysis of brazed joints between carbon fiber reinforced SiC composite and titanium alloy with TiC** CUI Bing, HUANG Jihua, XIONG Jinhui, ZHANG Hua (School of Materials Science and Engineering, University of Science and Technology Beijing, Beijing 100083, China). pp 85 – 88

**Abstract:** Carbon fiber reinforced SiC (C<sub>f</sub>/SiC) composite was successfully joined to titanium alloy with Ag-Cu-Ti-(Ti + C) mixed powder under proper parameters. The interfacial microstructure was examined with scanning electron microscope (SEM), energy dispersive spectrometer (EDS) and X-ray diffraction (XRD), and the mechanical properties of the brazed joints were tested. The results showed that Ti in the powder reacted with the composite during brazing, the resultant joints mainly consisted of TiC, Ti<sub>3</sub>SiC<sub>2</sub>, Ti<sub>5</sub>Si<sub>3</sub>, Ag, TiCu, Ti<sub>3</sub>Cu<sub>4</sub> and Ti<sub>2</sub>Cu phases. The dense bonding layers formed and were reinforced by TiC in situ synthesized from the reaction between C and Ti in the filler materials. The TiC particulates obviously relieved the thermal stress in the heterogeneous joint, resulting in an increase in shear strength of the brazed joint. The maximum shear strengths of the brazed joints at room temperature, 500 °C and 800 °C reached 145 MPa, 70 MPa and 39 MPa, respectively, which were remarkably higher than those brazed with C<sub>f</sub>/SiC/Ag-Cu-Ti/TC4.

**Key words:** C<sub>f</sub>/SiC composite; Ti alloy; brazing; TiC

**Reactive contact brazing between aluminium alloy and copper by high frequency induction method** ZHANG Hongtao, LIU Duo, FENG Jicai, HU Leliang (School of Materials Science and Engineering, Harbin Institute of Technology (Weihai), Weihai 264209, China). pp 89 – 92

**Abstract:** High-frequency induction contact reactive brazing of 6063 aluminium alloy to pure copper was investigated in this paper. The composition of the brazing flux was optimized according to the brazing process and mechanical properties of the resultant joints. The interfacial microstructure and phase constitution of the joint was analyzed by means of SEM and EDS. The results showed that the joint made with the flux of 65% ZnCl<sub>2</sub> + 10% NaCl + 25% NH<sub>4</sub>Cl was better than the joints made with the other two fluxes. The thickness of the brazing seam was about 80 μm and the interface mainly consisted of Al solid solution and Al<sub>2</sub>Cu phases, and massive Zn and Na elements diffused into the seam. The maximum shearing strength of the joint reached 58 MPa.

**Key words:** aluminium alloy; pure copper; contact reactive brazing; interfacial structure

**Effect of sodium molybdate on corrosion behavior of 2024 and its weld joint by FSW** SHEN Changbin<sup>1,2</sup>, CHEN Ying<sup>1</sup>, GE Jiping<sup>1,2</sup> (1. Liaoning Key Materials Laboratory for Railway, Dalian Jiaotong University, Dalian 116028, China; 2. School of Materials Science and Engineering, Dalian Jiaotong University, Dalian 116028, China). pp 93 – 96

**Abstract:** In this paper, 2024 aluminum alloy was friction stir welded. In the ambient mixed solution of 0.2 mol/L NaHSO<sub>3</sub> and 0.6 mol/L NaCl with the addition of different concentrations of sodium molybdate (Na<sub>2</sub>MoO<sub>4</sub>), the effect of Na<sub>2</sub>MoO<sub>4</sub> on the corrosion behavior of the friction stir weld and